

# An Iterative Method for Constructing Equilibrium Phase Models of Stellar Systems

S.A. Rodionov<sup>1\*</sup>, E. Athanassoula<sup>2</sup> and N.Ya. Sotnikova<sup>1</sup>

<sup>1</sup>*Sobolev Astronomical Institute, St. Petersburg State University, Universitetskij pr. 28, 198504 St. Petersburg, Stary Peterhof, Russia*

<sup>2</sup>*Laboratoire d'Astrophysique de Marseille (LAM), UMR6110, CNRS/Université de Provence, Technopôle de Marseille-Etoile, 38 rue Frédéric Joliot Curie, 13388 Marseille Cédex 20, France*

Accepted ???? ???. Received ???? ??? ??. in original form ???? ??? ??

## ABSTRACT

We present a new method for constructing equilibrium phase models for stellar systems, which we call the iterative method. It relies on constrained, or guided evolution, so that the equilibrium solution has a number of desired parameters and/or constraints. This method is very powerful, to a large extent due to its simplicity. It can be used for mass distributions with an arbitrary geometry and a large variety of kinematical constraints. We present several examples illustrating it. Applications of this method include the creation of initial conditions for  $N$ -body simulations and the modelling of galaxies from their photometric and kinematic observations.

**Key words:** galaxies: kinematics and dynamics – methods:  $N$ -body simulations

## 1 INTRODUCTION

In astronomy there are at least two problems where equilibrium phase models of stellar systems need to be constructed. The first one is the construction of phase models for real galaxies from observational data, i.e. the modelling of observational data. The second problem is the construction of initial conditions for  $N$ -body simulations of stellar systems. It is obvious that these two problems are tightly connected, and yet they have, so far, been solved by different methods. The Schwarzschild method (Schwarzschild 1979) and its modifications is often used for modelling of observational data (e.g. Häfner et al. 2000; van den Bosch et al. 2006; Thomas 2007; van den Bosch et al. 2008; de Lorenzi et al. 2008), but has almost never been used so far to produce initial conditions for simulations. For  $N$ -body initial conditions, a wide variety of methods has been used, based on the Jeans theorem (e.g. Zang 1976; Athanassoula & Sellwood 1986; Kuijken & Dubinski 1995; Widrow & Dubinski 2005; McMillan & Dehnen 2007), or on Jeans' equations (e.g. Hernquist 1993). In the case of multi-component systems, e.g. disc galaxies with a bulge and a halo, the components are built separately and then either simply superposed, or the potential of the one is adiabatically grown in the other (e.g. Barnes 1988; McMillan & Dehnen 2007; Athanassoula 2007) before superposition.

For real galaxies the phase space density is generally unknown, but we do have some information about it. For example, we know more or less accurately a distribution of

mass for the visible components (notwithstanding uncertainties due to the mass to light ratio) and we often have some constraints on the velocity distribution. It is also reasonable to assume that the galaxy is in an equilibrium state. So in general, the problem of constructing a model in phase space is equivalent to constructing an equilibrium phase model with a given mass distribution and, in many cases, given kinematic constraints. In the case of modelling observational data (first of the two above mentioned problems) the kinematic parameters are the observed velocities integrated along the line of sight. In the case of initial conditions for  $N$ -body simulations, a wide variety of kinematic parameters is possible, depending on the problem the simulation addresses.

We have developed a new method for constructing equilibrium phase models with a given mass distribution and with given kinematic parameters, which we call the iterative method. It can be applied to systems with arbitrary geometry, so that the requested mass distribution can be arbitrary. The idea and a first implementation was presented in Rodionov & Sotnikova (2006). In Rodionov & Orlov (2008) we improved it, and applied it to construct an  $N$ -body model of the stellar disk of our Galaxy for two realistic mass models of the Milky Way. Here we present a final version of this method, fully allowing kinematical constraints. In the previous articles we had concentrated on constructing equilibrium phase models with a given mass distribution, so that kinematic parameters were either not considered or only in terms of auxiliary parameters, such as the total angular momentum (Rodionov & Sotnikova 2006; Rodionov & Orlov 2008). This, however, limited the applicability of our method, both

\* E-mail: seger@astro.spbu.ru

for initial conditions and for modelling real galaxies. Indeed, initial kinematics play a crucial role in determining the evolution of  $N$ -body systems, while observational constraints more often than not include kinematics. In this paper we give equal attention to the mass distribution and kinematical constraints, so that the iterative method can now be used for a number of interesting applications. In principle, in our method, both the kinematic constraints and the mass distribution can be arbitrary. But the part of our algorithm that concerns the kinematic constraints is not universal, contrary to the part that handles the mass distribution, but is tailored to the specific constraint. Here we consider several types of constraints. Once these are understood, it is rather easy to extend the algorithm for every new type of kinematic parameter (see below).

The power of the iterative method stems from its simplicity. The iterative method is based on a simple and, in a way, obvious idea, which is implemented in a simple algorithm. The purpose of this article is to fully describe this method. We first introduce the basic concept in Section 2, where we also explain the different modules of the algorithm and the way they should be applied. In section 3 we illustrate the use of the method with three examples, namely a triaxial system, a multi-component model of a disk galaxy (including live disk, bulge and halo components) and a disk constructed with given line-of-sight kinematic. We briefly conclude in section 4.

## 2 THE ITERATIVE METHOD

### 2.1 General Idea of the Iterative Method

The aim of the iterative method is to construct equilibrium  $N$ -body models with a given mass distribution and with given kinematic properties, parameters, or constraints. This method relies on the fact that any non-equilibrium system will tend, more or less fast, to a stable equilibrium. We thus start by constructing any arbitrary, non-equilibrium  $N$ -body system, and let it evolve. Such an evolution changes both its mass distribution and its kinematics, so that the final system does not have the desired properties. To achieve the latter, we developed a new method which we call the iterative method and which relies on a constrained, or guided, evolution. We will describe it fully in this section. This idea is of course applicable for any arbitrary dynamical system and is even widely used in every day life.

To give an example, let us consider a donkey walking by itself in a field. After some time the donkey can be anywhere in the field. Now consider another donkey which we attach to a tree by a rope. This donkey also walks in the field, but it will have to stay inside a circle of radius equal to the length of the rope. This is an example of a constrained evolution, which will necessarily lead to a final state within a circle around the tree. The crucial point now is how to achieve this constraint, i.e. what will the equivalent of the rope be in the case of galaxy models.

The general scheme of our method is presented in Fig. 1 and can be applied to any arbitrary dynamical system. Let our task be to find an equilibrium state of some dynamical system obeying given constraints or having specific values of some given parameters. We start from any arbitrary state of

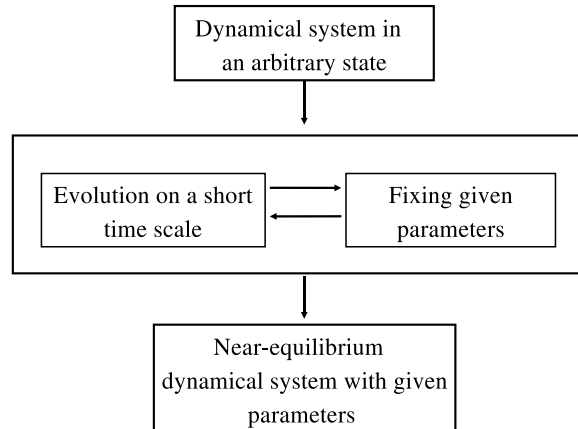


**Figure 1.** General scheme of the iterative method in the case of an arbitrary dynamical system.

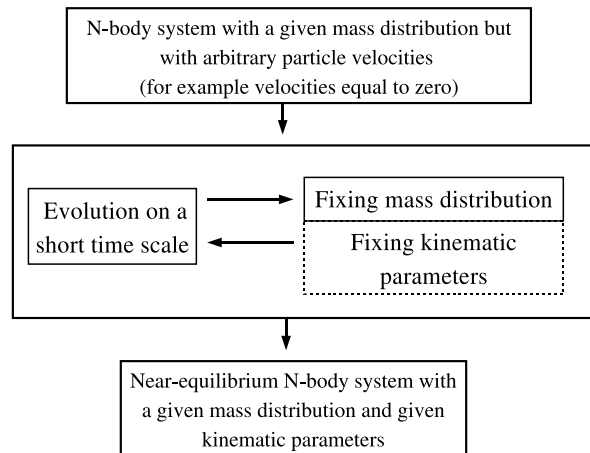


**Figure 2.** The scheme of the iterative method for the case of an  $N$ -body system with a given mass distribution and given kinematical parameters.

our dynamical system and allow the system to evolve during a short time interval. We then need to make sure that the given parameters have the required values. In order to achieve this we need to modify the system so that the given parameters have the necessary values, while making sure that the other quantities or parameters are kept unchanged, so as to retain memory of the evolution. As shown in Fig. 1, we iterate these two steps, alternating short evolutions and modifications of the system to fix the set parameters. We thus constrain the evolution in order for it to reach an equilibrium state with the desired set of constraints. We stop when we consider we are sufficiently near the desired equilibrium state of the system.

Let us now consider a case, in which we wish to construct an equilibrium  $N$ -body system with a given mass distribution and with or without given kinematic constraints. The scheme is outlined schematically in Fig. 2. We initially create an  $N$ -body system with a given mass distribution but with arbitrary particle velocities (for example velocities equal to zero). We then start the iterative procedure,

by letting the system go through a sequence of evolutionary steps of short duration. At the end of each one of these steps, and before the new step is started, we need to set the appropriate parameters. Let us first consider the case where we wish to have a specific mass distribution, but have no kinematic constraints. To achieve this, we construct a new  $N$ -body system, with the desired mass distribution but with velocities chosen according to the velocity distribution obtained from the evolution. In other words, we “transfer” the velocity distribution from the system obtained from the evolution to a new system, which will have the desired mass distribution and an evolved velocity distribution. The algorithm performing this “transfer” is the core of the iterative method, and will be discussed in more detail in section 2.2. If we have kinematic constraints as well, we need to modify the velocities of the particles in such a way that the constraints are fulfilled and, at the same time, as little as possible so that some memory of the evolution is kept. How this is done in practise depends on the imposed constraints and will be described, for a number of cases, in section 2.3. Procedures for further types of constraints can be easily found following similar techniques. In all cases we have a new system which has the desired mass distribution, obeys the necessary velocity constraints, while being nearer to equilibrium, since it retains partial memory of the evolution. We repeat this iterative procedure a number of times, alternating one evolution phase and one phase where the necessary parameters are set, until we come as near to the desired equilibrium state as desired.

## 2.2 Transfer of velocity distribution

The transfer problem can be formulated as follows. Any evolution step ends with a model, which we will refer to as the “old” model. This step is followed by a constraining, or fixing step, during which we create a “new” model with the desired mass distribution. We now need to transfer the velocity information from the “old” to the “new” model. There is more than one way to achieve this transfer. Rodionov & Sotnikova (2006) used an algorithm based on moments of the velocity distribution, which, however, proved to be rather complicated and cumbersome. Here we suggest a much simpler and more reliable algorithm, which is in fact an improvement of an algorithm initially used in Rodionov & Orlov (2008).

The basic idea of our velocity transfer algorithm is as follows. We assign to the new-model particles the velocities of those particles from the old model that are nearest to the ones in the new model. The simplest (although, as we show below, not necessarily optimum) implementation of this idea is evident. One can prescribe to each particle in the new model the velocity of the nearest particle from the old model. Let us formulate this proposition more strictly. For each  $i$ -th particle of the new model, one finds the  $j$ -th particle in the old model with the minimum value of  $|\mathbf{r}_i^{new} - \mathbf{r}_j^{old}|$ . Here,  $\mathbf{r}_i^{new}$  is the radius vector of the  $i$ -th particle in the new model, and  $\mathbf{r}_j^{old}$  is the radius vector of the  $j$ -th particle in the old model. Hereafter we will always imply this definition when we talk of the nearest or closest particle. One then takes as the velocity of the  $i$ -th particle in the new model the velocity of the  $j$ -th particle in the old model. This simple algorithm has, however, one essential drawback. If the numbers of particles in the old and new models are

the same then only about one-half of the particles in the old model participate in the velocity transfer. The reason is that many old-model particles transfer their velocities to several particles in the new model. As a result of this, almost one-half of the particles in the old model do not transfer their velocities at all. This means that a significant amount of information on the velocity distribution will be lost in the transfer process. The noise will therefore grow, as we verified in numerical experiments. Thus, this transfer algorithm is not optimum.

This shortcoming can, nevertheless, be overcome by modifying this transfer scheme. For this, we introduce an input parameter, which we call the “number of neighbours”  $n_{nb}$ . We also introduce, for each particle in the old model, the parameter  $n_{used}$ , which denotes the number of times this particle has been used for velocity copying. At the beginning of the transfer procedure we set  $n_{used} = 0$  for each particle in the old model, since its velocity information has not been yet transferred to any of the new model particles. For any given particle in the new model we find the nearest  $n_{nb}$  neighbours in the old model (the closeness being understood as defined above) and from these we single out the subgroup of particles that have a minimum  $n_{used}$ . From this subgroup we find the particle that is the closest one to the position of the new-model particle, add one to its  $n_{used}$  value and prescribe its velocity to the new-model particle we are examining.

We note that if  $n_{nb} = 1$  this algorithm is the same as the previous one and about half of the particles will not take part in the velocity distribution transfer. If, however, we take  $n_{nb} = 10$ , only a small fraction (a few per cent) of old-model particles will not take part in the transfer process. We adopt this improved transfer method since we showed that it gives good results in the iterative procedure.

If the desired model has some symmetry, it can be useful to take it into account in the algorithm of velocity transfer by redefining the distance between two particles. For example, if we wish to build an axisymmetric system, we search for the nearest particles in the two-dimensional space  $R - z$  (where  $R$  the cylindrical radius) instead of the three-dimensional space  $x - y - z$ . We then transfer the velocity of this nearest old-model particle (in cylindrical coordinates) to the new-model particle. It is important to adopt this new definition of the distance in order to fix not only the mass distribution, but also fix the velocity distribution and to make it fully axisymmetric.

We have thus introduced three variants of the velocity transfer algorithm. We will refer to them as “transvel\_3d”, “transvel\_cyl” and “trasvel\_sph”.

(i) “transvel\_3d”: This is the basic algorithm, for the case when the desired system has no assumed symmetry. By using this algorithm in the iterative method we only fix the mass distribution and leave the velocity distribution unchanged. In the current work we use this algorithm when constructing triaxial models.

(ii) “trasvel\_cyl”: This is a modification of the basic algorithm for axisymmetric systems and was described just above. We use this algorithm when both the desired mass and velocity distribution are axisymmetric. In the current work we use this algorithm for constructing all models except for the triaxial ones.

(iii) “transvel\_sph”: This is a modification of the basic algorithm for spherical systems. In this version of the algorithm we search for the nearest particles in one dimensional “ $r$ ” space, where  $r$  is the spherical radius. By using this algorithm in the iterative method we fix both the mass and the velocity distribution to make the system fully spherically symmetric. This was used in Sotnikova & Rodionov (2008).

### 2.3 Fixing the Kinematic Parameters

Here we describe algorithms for fixing different kinematic parameters. The general algorithm is as follows. We slightly change the particle velocities to fix given kinematic parameters, but we keep as many other parameters as possible unchanged. Here we describe in detail only a number of algorithms, which we use in this paper. But it is easy to develop algorithms for any other kinematic parameter. It is only necessary to follow the general principle: “keep unchanged the parameters that do not need to be fixed”.

#### 2.3.1 Fixing the radial velocity dispersion profile $\sigma_R(R)$

We use this algorithm in order to fix in stellar disks the radial velocity dispersion profile to a given function  $\sigma_R(R)$  (for an application, see section 3.2).

Let  $\sigma_R(R)$  be the given radial velocity dispersion profile which we want to fix, where  $R$  is the cylindrical radius. After each evolutionary step (see Sect.2.1) we need to change slightly the radial velocities of particles in order to fix this profile. The model is divided into  $n_{\text{div}}$  concentric cylindrical annuli, each containing the same number of particles. For each annulus  $j$ , we calculate the target value of the radial velocity dispersion

$$\sigma_R^j = \sigma_R(R_j), \quad (1)$$

where  $R_j$  is the mean value of the  $R$  coordinate of all particles in part  $j$ . The new radial velocity of the  $i$ -th particles in the  $j$  region is then prescribed as follows.

$$v_{Ri} = v'_{Ri} \sigma_R^j / \sigma_R^{j'}, \quad (2)$$

where  $v'_{Ri}$  is the current value of the  $i$ -th particle radial velocity,  $v_{Ri}$  is the corrected  $i$ -th particle radial velocity and  $\sigma_R^{j'}$  is the current value of radial velocity dispersion in part  $j$ . We note that in this scheme we have assumed that the mean radial velocity is equal to zero.

#### 2.3.2 Fixing the radial anisotropy profile

This algorithm is very similar to previous one and is very useful for building spherical models with a given profile of velocity anisotropy. We will use it for building the halo model in section 3.2 and it has also been used in Sotnikova & Rodionov (2008).

Let  $\sigma_\theta$ ,  $\sigma_\varphi$  and  $\sigma_r$  be the velocity dispersions in the  $\theta$ ,  $\varphi$  and  $r$  directions of spherical coordinate system and let us aim e.g. for a model with a given profile,  $\beta(r)$ , of the  $\sigma_\theta/\sigma_r$  ratio. The model is divided in concentric spherical shells, each containing the same number of particles. For each shell  $j$ , we calculate the target value of  $\sigma_\theta/\sigma_r$

$$\beta_j = \beta(r_j), \quad (3)$$

where  $r_j$  is the mean value of the  $r$  coordinate of all particles in shell  $j$ . We will attempt to obtain this ratio by changing appropriately the  $\theta$  component of particle velocities (alternatively, we could have changed the  $r$  component). The new  $\theta$  velocity component of the  $i$ th particle in the  $j$ th region will then be prescribed by

$$v_{\theta i} = v'_{\theta i} \beta_j \frac{\sigma_r^{j'}}{\sigma_\theta^{j'}}, \quad (4)$$

where  $v'_{\theta i}$  and  $v_{\theta i}$  are, respectively, the current and the corrected values of the  $i$ -th particle  $\theta$  velocity component and  $\sigma_r^{j'}$  and  $\sigma_\theta^{j'}$  are the current values of the radial and  $\theta$  velocity dispersion, respectively, in part  $j$ .

#### 2.3.3 Fixing the line-of-sight mean velocity or the line-of-sight velocity dispersion in the case of an edge-on disk

In this section, we describe two algorithms, one for fixing the line-of-sight mean velocity and the other for fixing the line-of-sight dispersion of an axisymmetric disk. To set the notation, let us assume that the stellar disk rotates about the  $z$ -axis, the disk plane lies in the  $(x, y)$  plane and the line of sight is along the  $y$  axis (edge-on disk). We invert the sign of  $v_y$  for each particle with  $x < 0$  in order to make the half disk with  $x < 0$  kinematically identical to the half with  $x > 0$  and flip the  $x < 0$  particles on the  $x > 0$  part. We then divide the disk in slits parallel to the  $(y, z)$  plane and at different distances from the centre, i.e. at different values of  $x$ , in such a way that all slits have the same number of particles.

Let us denote by  $\bar{v}_{\text{los}}(x)$  the desired profile of the line-of-sight mean velocity, i.e. the mean value of  $v_y$  after integration along the line of sight. For each slit  $j$  we calculate the target value of the line-of-sight mean velocity  $\bar{v}_{\text{los}}^j = \bar{v}_{\text{los}}(x_j)$  (where  $x_j$  is the mean value of  $|x|$  for particles in part  $j$ ) and the current value of the line-of-sight mean velocity  $\bar{v}_{\text{los}}^{j'}$  (as the mean value of  $v_y$  for all particles in slice  $j$ ). The new  $y$  velocity component of particle  $i$  in region  $j$  should then be

$$v_{yi} = v'_{yi} + (\bar{v}_{\text{los}}^j - \bar{v}_{\text{los}}^{j'}), \quad (5)$$

where  $v'_{yi}$  is the current value of the  $i$ -th particle  $y$  velocity and  $v_{yi}$  is the corrected  $i$ -th particle  $y$  velocity. Particles which were flipped to  $x > 0$  part have to be flipped back and the sign of their  $y$  velocity component reversed. The particles are then azimuthally mixed to make the velocity distribution axisymmetric and the step is concluded. Of course, in this way we have tampered with  $v_{\text{los}}$ , but this unavoidable. Nevertheless, after a number of iterations, both the axisymmetry and the desired  $v_{\text{los}}$  will be achieved.

The algorithm for fixing  $\sigma_{\text{los}}(x)$  is very similar, except that we have to calculate in each slit the current value of the line-of-sight velocity dispersion  $\sigma_{\text{los}}^{j'}$  as the dispersion of  $v_y$  for all particles in slit  $j$ . Let  $\sigma_{\text{los}}(x)$  be the desired profile of the line-of-sight velocity dispersion. In order to achieve this, the new  $y$  velocities should be modified as follows

$$v_{yi} = (v'_{yi} - \bar{v}_{\text{los}}^{j'}) \frac{\sigma_{\text{los}}^j}{\sigma_{\text{los}}^{j'}} + \bar{v}_{\text{los}}^{j'}, \quad (6)$$

where  $\bar{\sigma}_{\text{los}}^j = \sigma_{\text{los}}(x_j)$  is the target value of the line-of-sight velocity dispersion. We note that in this algorithm we have

to take into account that the value of  $\bar{v}_{\text{los}}^{j'}$  need not necessarily be equal to zero. As previously, we still have to flip back particles which were flipped to the  $x > 0$  part, invert the sign of their  $y$  velocity component with and mix the particles azimuthally.

#### 2.3.4 Fixing velocity isotropy conditions

An isotropic velocity distribution depends only on the velocity module and not on the direction of the velocity. Our algorithm for fixing it is very simple. For each particle, we keep the velocity module unchanged and randomise its direction, thus ensuring that the velocity distribution is isotropic. For spherical isotropic models, the distribution function (DF) is known, at least formally, or numerically. Thus the construction of such models can be considered as a test of the iterative method, and we have verified in a number of cases that the models constructed by the iterative method are identical to the models constructed by using known equilibrium DF. The construction of spherical isotropic models with the iterative method was first described in Rodionov & Sotnikova (2006). That work, however, used an old and rather complicated algorithm for transferring the velocity distribution. Here we use a different, superior algorithm, based on the description in Sect. 2.2. We again made sure that the models thus constructed are identical to the models obtained by using a known DF. Furthermore, we also used this algorithm for constructing models which are not fully isotropic models, but rather not-very-far from isotropic (see section 3.1 and 3.2).

#### 2.4 How many parameters should we fix?

The goal of the iterative method is to construct equilibrium  $N$ -body models with given parameters (i.e. with a given mass distribution and with given kinematic constraints). There are in general three possible cases with respect to the number of constraints.

In the first case the number of given parameters, or constraints are such that only one equilibrium model can exist. In this case, we can expect that the iterative method will converge to this unique equilibrium model, independent of the initial state from which the iteration is started. For example, it is known that for a spherical model with a given mass distribution only one isotropic equilibrium DF exists. If we construct a spherical model by using the iterative method and we fix velocity isotropy as a kinematical constraint (section 2.3.4), then the iteration always converges to the same model, independent of the initial state, as expected.

In the second case, the number of give parameters is such that many equilibrium models can exist, i.e. this number is insufficient for determining uniquely the equilibrium model. In this case we can expect that the result of the iterative method will depend on the choice of the initial model. The iteration will converge to the equilibrium model which is “nearest” in some sense to the initial model. Alternatively, the iteration will converge to some specific, in some sense, model. For example, when constructing a triaxial model in section 3.1 we fix only the mass distribution and do not set any kinematic constraints. Of course in this case the result of the iterations will depend on the initial state (see

section 3.1 for details). Another, more involved, example is the construction of a disk model with given total angular momentum. In principle, many such equilibrium models are possible, yet the iterations of Rodionov & Orlov (2008) always converged to the same model. It is unclear why this is the case, but it could be due to a specificity of the model (see Rodionov & Orlov 2008 for details).

The last possibility is that for the adopted parameters, no equilibrium model exists, i.e. we have fixed too many parameters. In this case the iteration will either not converge at all, or it will converge to a system with the parameters we have fixed, which is in non-equilibrium, but close in some sense to equilibrium.

#### 2.5 Technical comments

In this section we elaborate a few important technical points, useful for anybody wishing to apply the iteration method.

One of the free parameters of the iterative method is the duration  $t_i$  of each iteration, i.e. the time interval over which the system is evolved during each iteration. How should the numerical value of  $t_i$  be chosen? It is clear that this time should not be too short, so as to allow the system to evolve sufficiently during one iteration step. On the other hand, it should not be too long either, so as not to permit the evolution of various instabilities; otherwise, these instabilities may change the system substantially. For example, when constructing a disk system it is necessary to use iteration steps considerably shorter than the growth time of the bar instability, which of course varies strongly from one model to another. For this reason, there is no strict criterion and  $t_i$  should be chosen empirically. Our experiments have shown that it is usually better to try relatively big  $t_i$  values, thus ensuring a much faster convergence. Moreover, in some situations the iterations for relatively small  $t_i$  don’t converge at all, while iterations for relatively big  $t_i$  do. This was, for example, the case when we constructed a model with relatively cold stellar disk. So if iterations don’t converge or they converge too slowly, it is often useful to consider bigger  $t_i$  (within of course reasonable limits). Examples of appropriate  $t_i$  values are given in all examples in Sect. 3. Moreover, our simulations have shown that, if we take  $t_i$  within reasonable limits, the result of the iteration is the same (within the noise limits) and independent of  $t_i$ , provided of course the chosen number of parameters and constraints allow a single solution. If the latter is not the case, and the result of the iteration depends on its starting model, then of course the result can depend also on  $t_i$ .

Another parameter of the iterative method is the parameter  $n_{nb}$  in the algorithm of velocity transfer (see section 2.2). Its value has been chosen in a more or less “ad hoc” manner and, by trial and error, we have found that a value of  $n_{nb} = 10$  is often satisfactory. Our test simulations have shown that the results of the iterative method for  $n_{nb} = 10$  and  $n_{nb} = 100$  are practically the same, at least for a total number of particles as those used in our trials, i.e. of the order of a few hundred thousands to a couple of millions.

The most computer costly part of our method is the computing of the evolution of the system in each iteration, since the computing cost of all other parts of the method is very small. For this reason it is recommended to use a

fast  $N$ -body code and we have adopted `gyrfalcON` (Dehnen 2000, 2002). Furthermore, our test simulations have shown that computation of the evolution can be carried out with relatively low accuracy. This is mainly due to the fact that we need to calculate the evolution only during short time intervals, so that errors do not have sufficient time to accumulate. Therefore, in the iterative method we use `GyrfalcON` with relatively big values of the tolerance parameter  $\theta_t$  and of the time-step (see section 3). Usually the total computing cost is considerably smaller, but still of the same order as that necessary to run a simulation with the constructed model. This of course will depend on whether we can start the iterations from a model reasonable close to the final one, or whether lack of any a priori knowledge leads us to start, e.g. from zero initial velocities. A ‘trick’ which helps reducing the computing cost is to make a few iterations initially with a small number  $N$  of particles and then gradually increase  $N$  to the required number. In the procedure of velocity transfer described in section 2.2 the number of particles in the old and the new system can be different. So in the next iteration step we can get a system with a larger number of particles.

### 3 EXAMPLES OF MODELS

In this section we consider three examples of models constructed by our method, namely a triaxial model of a spheroid, a multi-component model of a disk galaxy and a model with given line-of-sight kinematics.

#### 3.1 Triaxial model

Our first example is that of a triaxial model. As mass distribution we use a Plummer sphere flattened in two dimensions.

$$\rho(x, y, z) = \frac{3M_{\text{pl}}}{4\pi abc} a_{\text{pl}}^2 \left( \frac{x^2}{a^2} + \frac{y^2}{b^2} + \frac{z^2}{c^2} + a_{\text{pl}}^2 \right)^{-5/2}, \quad (7)$$

where  $M_{\text{pl}}$  and  $a_{\text{pl}}$  are the total mass and the scale-length of the model and  $a, b, c$  are rescaling parameters. In the present specific example we discuss a model with the following parameters:  $M_{\text{pl}} = 1$ ,  $a_{\text{pl}} = 3\pi/16$ ,  $a = 1$ ,  $b = 0.8$  and  $c = 0.7$ . Scaling our model to an elliptical galaxy with  $a = 3$  kpc and  $M_{\text{pl}} = 10^{11} M_{\odot}$ , gives a time unit  $t_u \approx 17$  Myr.

Our target is to construct an equilibrium  $N$ -body system with this given mass distribution. We didn’t impose any well-defined restriction on the kinematics of the system, but aimed instead for a velocity distribution not very far from isotropic. Our initial model was cold with velocities equal to zero. Our target model was reached in 50 iterations. For the first 10 we fixed a condition of velocity isotropy (section 2.3.4), while for the last 40 we didn’t fix any kinematic parameters. If we performed all 50 iterations without fixing any kinematic parameters, we would also obtain an equilibrium model but with a higher degree of anisotropy. We chose  $N = 500\,000$  and an iteration time  $t_i = 10$ . The integration step and the softening length were taken  $dt = 1/2^7$  and  $\epsilon = 0.01$ , respectively. The tolerance parameter for `gyrfalcON` was set to  $\theta_t = 0.9$  (see section 2.5) and we used the ‘`transvel3d`’ modification of the algorithm of velocity transfer (see section 2.2).

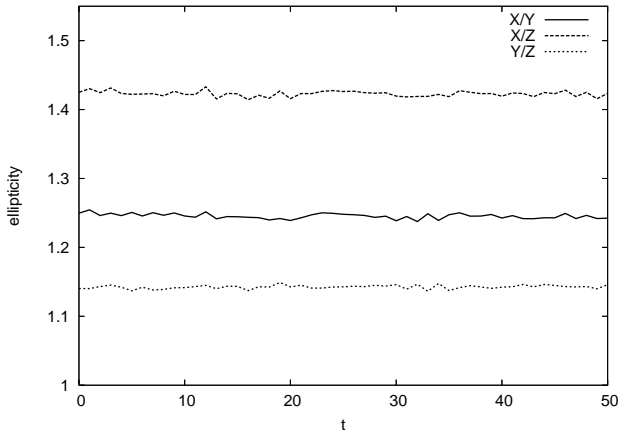


**Figure 3.** Evolution of the ellipticity for the three projections of the triaxial model constructed with our iterative method. Note that they do not evolve, i.e. that the model is in equilibrium.

In such a case it is crucial that the final model be sufficiently close to equilibrium so that the axial ratios do not tend to unity after some time evolution, as it happens for many other techniques used in calculating triaxial equilibria. To test this we evolved our model for 50 time units, i.e. roughly 50 crossing times for the scale-length of the system  $a_{\text{pl}}$ . The integration step and softening length were taken  $dt = 1/2^8$  and  $\epsilon = 0.005$ , respectively – in agreement with the recommendations of Rodionov & Sotnikova (2005) (see also Athanassoula et al. 2000) – and the tolerance parameter for `gyrfalcON` was set to  $\theta_t = 0.6$ . Fig. 3 shows the evolution of the ellipticity of the model for three different projections. This was calculated as the ratio of the medians of the absolute values of corresponding particle coordinates. As can be seen, the shape of the model is practically unchanged during the evolution. We also made sure that the model also conserved all its other properties, thus demonstrating that it is indeed very close to equilibrium.

#### 3.2 Multi-Component model of a disk galaxy

As a second example, we constructed a model of a disk galaxy consisting of three components: a stellar disk with a given profile of radial velocity dispersion, a non-spherical bulge and a halo with a given anisotropy profile.

To start, we need to define the mass distribution in each of the components. The disk model is an exponential disk with density:

$$\rho_d(R, z) = \frac{M_d}{4\pi R_d^2 z_0} \exp\left(-\frac{R}{R_d}\right) \text{sech}^2\left(\frac{z}{z_0}\right), \quad (8)$$

where  $M_d$  is the total disk mass,  $R_d$  is the disk scale length,  $z_d$  is its scale height and  $R$  is the cylindrical radius. The halo model is a truncated NFW halo (Navarro et al. 1996)

$$\rho_h(r) = C_h \frac{\exp(-r^2/r_{\text{th}}^2)}{(r/r_h)(1+r/r_h)^2}, \quad (9)$$

where  $r_h$  is the halo scale length,  $C_h$  is a parameter defining the mass of the halo and  $r_{\text{th}}$  is the truncation radius of the halo. For the bulge we used a truncated and flattened Hernquist sphere (Hernquist 1990) with density

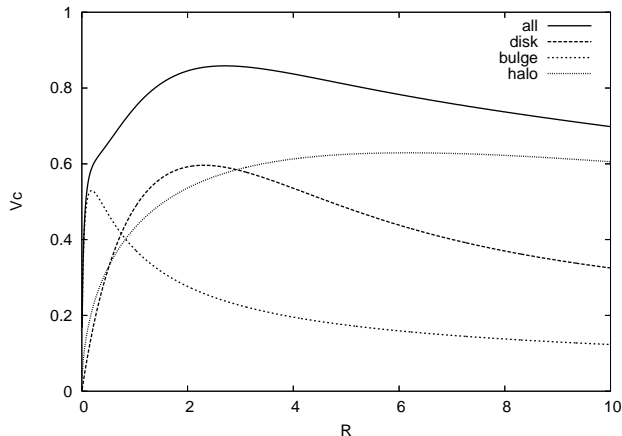


**Figure 4.** Rotation curve for the disk galaxy model. The solid line is the total rotation curve. We also show the contributions from the disk, halo and bulge components.

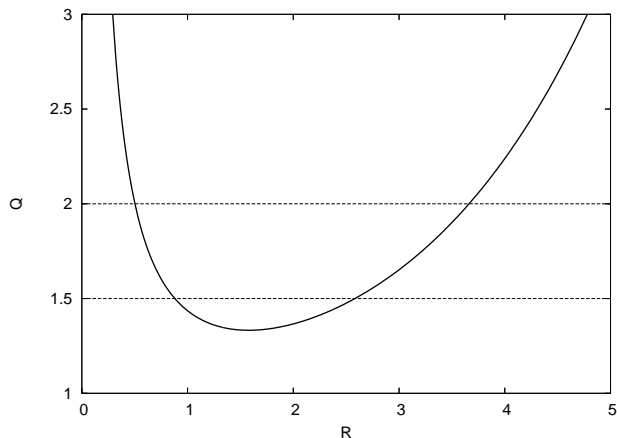


**Figure 5.** Radial profile of the Toomre parameter  $Q$  for the disk in the model described in Sect. 3.2.

$$\rho_b(R, z) = \frac{M'_b r_b \exp(-d^2/r_{tb}^2)}{2\pi q d(d+r_b)^3}, \quad (10)$$

where

$$d = \sqrt{R^2 + \frac{z^2}{q^2}}, \quad (11)$$

$r_b$  is the bulge scale length,  $M'_b$  is the total bulge mass before truncation,  $r_{tb}$  is the truncation radius of the bulge and  $q$  is the flattening parameter.

For the parameter values we chose for the disk:  $M_d = 1$ ,  $R_d = 1$ ,  $z_0 = 0.2$ , for the halo:  $r_h = 4$ ,  $C_h = 0.01$ ,  $r_{th} = 14$  and for the bulge:  $r_b = 0.2$ ,  $M'_b = 0.2$ ,  $r_{tb} = 2$ ,  $q = 0.7$ . For these parameters the total mass of the bulge and of the halo are  $M_b \approx 0.15$  and  $M_h \approx 4.98$ , respectively. We use units such that the constant of gravity is  $G = 1$ . Scaling our model to a disk galaxy with  $R_d = 3.5$  kpc and  $M_d = 5 \cdot 10^{10} M_\odot$ , gives a time unit  $t_u \approx 13.8$  Myr and a velocity unit  $v_u \approx 247.9$  km/s. The rotation curve for our model is shown in Figure 4, which also displays the contribution of the disk, halo and bulge components separately.

To make the exercise more realistic, we still need to

choose kinematical constraints for each of the components, although, as we have already mentioned, these are not obligatory for our method. We created the disk with the following profile

$$\sigma_R(R) = 0.3 \cdot \exp(-R/3) + 0.2 \cdot \exp(-R/0.5), \quad (12)$$

where  $\sigma_R$  is the radial velocity dispersion. From the mass model of the galaxy and from profile (12) we can calculate the radial profile of the Toomre parameter  $Q$  (Toomre 1964), shown in figure 5. Our main target here is to demonstrate that our method can construct an equilibrium model of the disk with any realistic profile of  $\sigma_R(R)$ . The choice of profile in eq. (12) is more or less arbitrary, but demonstrates that our method can work with more elaborate profiles than a single exponential function.

When constructing the bulge, we did not impose any specific kinematic constraints. Instead, we aimed for a model not-very-far from isotropic, as in the case of the triaxial model of Sect. 3.1.

For the halo we adopted a velocity anisotropy profile, so as to test a different kind of constraint. More specifically we chose

$$\frac{\sigma_\theta(r)}{\sigma_r(r)} = \frac{0.2}{\sqrt{\left(\frac{r}{0.9}\right)^2 + 1}} + 0.8, \quad (13)$$

where  $\sigma_\theta$  and  $\sigma_r$  are the velocity dispersion in the  $\theta$  and the  $r$  direction in a spherical coordinate system. Note that we constructed the phase model of the halo in the presence of the non-spherical potential of the disk and bulge, i.e. we don't have spherical symmetry and in the halo equilibrium model  $\sigma_\theta$  should not be equal to  $\sigma_\varphi$  (the velocity dispersion in  $\varphi$  direction). So when we constructed the halo model we fixed only the fraction  $\sigma_\theta/\sigma_r$ , but did not fix the fraction  $\sigma_\varphi/\sigma_r$ . This is different from the case of the isolated spherical NFW halo, constructed in Sotnikova & Rodionov (2008). And again we want to underline that kinematical constraints are not obligatory. We could also construct the halo, or the bulge, without any kinematical constraints, or with another type of kinematical constraints. For example we can construct a rotating halo with given total angular momentum or a rotating halo with a given profile of the mean azimuthal velocity.

Once the mass models and the required kinematical parameters for each of three components are defined, we can apply the iterative method for constructing an equilibrium  $N$ -body model for the whole system. In this specific example we chose  $N_d = 200000$ ,  $N_b = 30324$ ,  $N_h = 995978$  for the number of particles in disk, bulge and halo, respectively. With these numbers, the mass of particles in all components is the same. We constructed each of these components separately in the rigid potential of all other components. In order to take into account the external potential, we need to make only one small evident modification of the iterative method. Namely, when we need calculate the evolution of the system during the iteration time (see fig. 2), we simply need to do it in the presence of the external potential. This can be done either by introducing an analytical external potential to the *gyrfalcON* program, or we can add it as a rigid  $N$ -body system. In current work we use the latter. For example, in order to add a rigid halo we simply add in the system rigid particles according to the mass distribution of the halo.

Let us first describe the disk construction. Our initial model was a cold disk where all particles move on circular orbits. Indeed, the circular velocity can be easily calculated, since the mass distribution in the model is known. Had we, instead, started off with zero disk velocities, we would have again obtained an equilibrium model, but with counter rotating subsystems. This will happen because we fix only the profile of  $\sigma_R(R)$  and do not fix any parameters defining the direction of rotation. It is therefore better to start off the iterations with a rotating disk, unless of course a disk with counter-rotating components is specifically sought. Note that the result of the iteration is independent of the initial iterative guess for the disk rotation. For example it will be the same if initially all the disk particles have tangential velocities equal to half of the circular velocity, or twice that.

We made 50 iterations, each with  $t_i = 20$ . The integration step and softening length were taken  $dt = 1/2^4$  and  $\epsilon = 0.04$ , respectively and the tolerance parameter for `gyrfalcON` was set  $\theta_t = 0.9$ . In order to fix the  $\sigma_R(R)$  profile we used the algorithm described in section 2.3.1. The number of layers in this algorithm was  $n_{\text{div}} = 200$  (see section 2.3.1). We used the “`transvel_cyl`” modification of the algorithm of velocity transfer (see section 2.2). This algorithm also was used for constructing the bulge and halo components. We call this disk model DISK.SVR.

For constructing the bulge we also made 50 iterations. The other parameters for this construction were  $t_i = 10$ ,  $dt = 1/2^6$ ,  $\epsilon = 0.02$  and  $\theta_t = 0.9$ . Our initial model was a cold model with velocities equal to zero. During the first 10 iterations we fixed a condition of velocity isotropy (section 2.3.4), while we did not set any kinematical constraints during the last 40 iterations.

To construct the halo we used again 50 iterations and the remaining parameters were taken as follows :  $t_i = 50$ ,  $dt = 1/2^4$ ,  $\epsilon = 0.04$  and  $\theta_t = 0.9$ . For fixing the velocity anisotropy radial profile (13) we used the algorithm described in section 2.3.2. The number of layers in this algorithm was  $n_{\text{div}} = 500$ .

Once all three components of our model were constructed, we simply stacked them in order to obtain the complete system. In order to check whether this was indeed near equilibrium, as it should, we simply evolved with a full  $N$ -body simulation, using again `gyrfalcON`, now with an integration step and softening length of  $dt = 1/2^7$  and  $\epsilon = 0.02$  (parameters were chosen according to recommendations of Rodionov & Sotnikova (2005)). The tolerance parameter for `gyrfalcON` was set  $\theta_t = 0.6$ . The evolution of the total system over 160 time units is illustrated separately for the disk, bulge and halo components in figures 6, 7 and 8, respectively. These show that all three components of the constructed model conserve their structural and dynamical properties very well, demonstrating that the constructed model is indeed close to equilibrium as it should.

An interesting question arises in connection with the equilibrium of our model: how well do the moments of the velocity distribution in the constructed disk satisfy the equilibrium Jeans equations (see Binney & Tremaine 1987)?

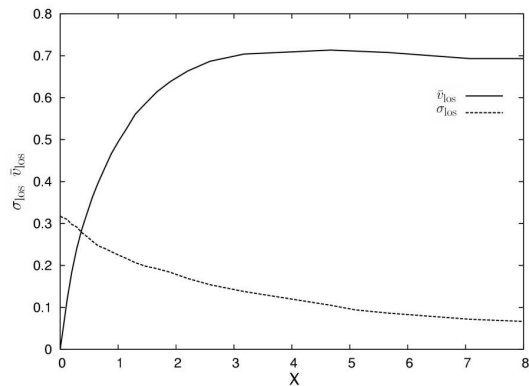


**Figure 10.** The edge-on line-of-sight mean velocity  $\bar{v}_{\text{los}}(x)$  and velocity dispersion  $\sigma_{\text{los}}(x)$  for model DISK.SVR. These parameters are defined in section 2.3.3.

$$\begin{cases} \bar{v}_\varphi^2 &= v_c^2 + \sigma_R^2 - \sigma_\varphi^2 + \frac{R}{\rho_d} \frac{\partial(\rho_d \sigma_R^2)}{\partial R}, \\ \sigma_\varphi^2 &= \frac{\sigma_R^2 R}{2\bar{v}_\varphi} \left( \frac{\partial \bar{v}_\varphi}{\partial R} + \frac{\bar{v}_\varphi}{R} \right), \\ \frac{\partial(\rho_d \sigma_z^2)}{\partial z} &= -\rho_d \frac{\partial \Phi_{\text{tot}}}{\partial z}. \end{cases} \quad (14)$$

Here  $\Phi_{\text{tot}}$  is the potential generated by all the components of our model (disk, halo and bulge),  $\bar{v}_\varphi$ ,  $\sigma_R$ ,  $\sigma_\varphi$  and  $\sigma_z$  are four moments of the velocity distribution in the disk (mean azimuthal velocity and velocity dispersions in the  $R$ ,  $\varphi$  and  $z$  directions, respectively).

Fig. 9 compares the radial profiles of  $\bar{v}_\varphi$ ,  $\sigma_\varphi$ , and  $\sigma_z$  calculated from the constructed disk and from the Jeans equations (14). It can be seen that the model follows the Jeans equations very well. Note that the moments of velocity distribution both in the Jeans equations and in the constructed disk depend on  $z$ . In fig. 9, all moments calculated by means of Jeans equations were calculated for  $z = 0$ . We thus took only particles with  $|z| < 0.05$  to calculate them from simulations. We also checked that our disk follows the Jeans equations very well in the rest part of the space (not shown here).

We want to underline that, according the Jeans equations, the  $\sigma_z(R, z)$  in our disk is unambiguously defined by the chosen mass model of the galaxy (see third equation of system (14)), as already discussed by Rodionov & Sotnikova (2006).

### 3.3 Models with given line-of-sight kinematics

In this section we demonstrate the capability of the iterative method to construct models with given line-of-sight kinematics. Let us first calculate the edge-on line-of-sight mean velocity  $\bar{v}_{\text{los}}(x)$  and the edge-on line-of-sight velocity dispersion  $\sigma_{\text{los}}(x)$  of the disk model constructed in the previous section (model DISK.SVR in section 3.2). These profiles are presented on figure 10.

We construct two disk models. The first one, called DISK.MVLOS, with a given  $\bar{v}_{\text{los}}(x)$  and the second one, called DISK.SVLOS, with a given  $\sigma_{\text{los}}(x)$ . Since we use the disk galaxy mass model described in the previous section, the process is similar to reconstructing DISK.SVR by using line-of-sight kinematic profiles obtained from “observation”.



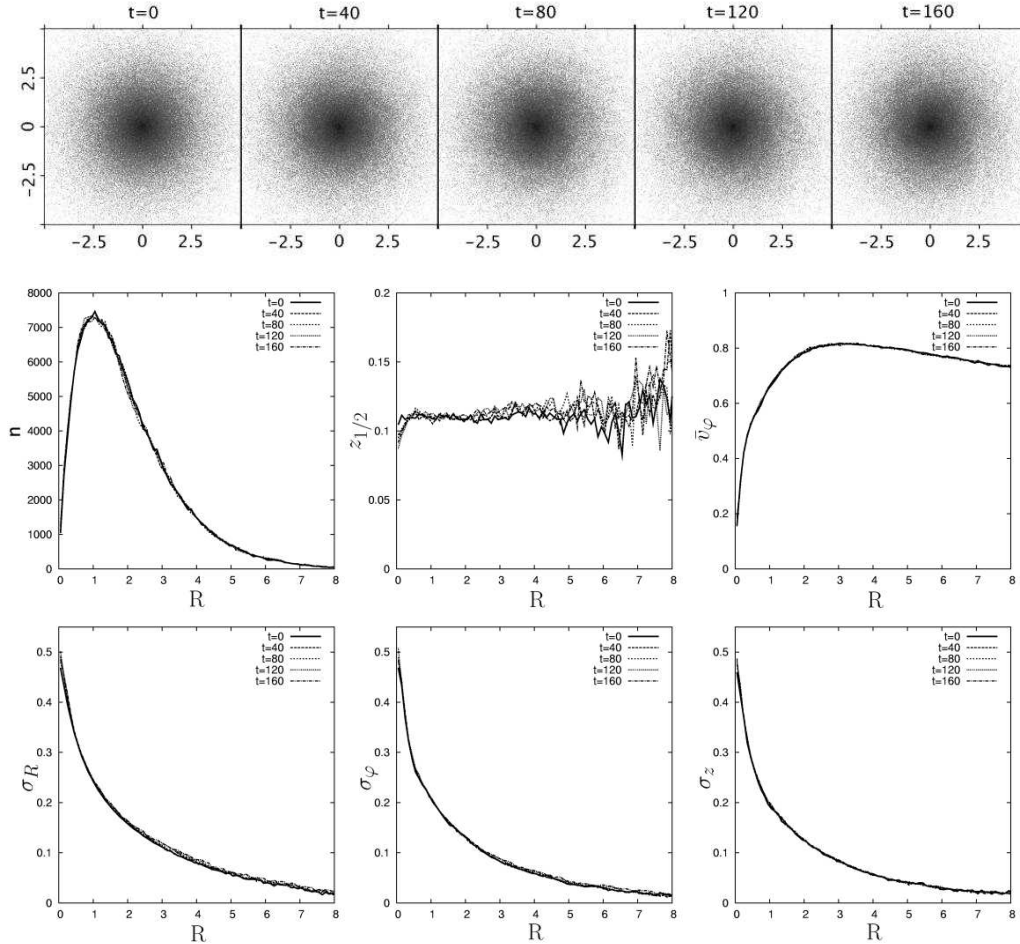


**Figure 6.** Initial evolutionary stages for the disk of the constructed disk galaxy model. The evolution of the model was calculated with live disk, halo, and bulge components (see also fig. 7 and 8). From left to right, the upper snapshots show the disc views face-on for times 0, 40, 80, 120 and 160 and the grey scales are logarithmically spaced. The middle and bottom panels show the dependence of various disc quantities on the cylindrical radius  $R$  at the same times. Here  $n$  is the number of particles in concentric cylindrical layers;  $z_{1/2}$  is the median of the value  $|z|$ , i.e a measure of the disc thickness (see Sotnikova & Rodionov 2006) and  $\bar{v}_{\varphi}$ ,  $\sigma_R$ ,  $\sigma_{\varphi}$  and  $\sigma_z$  are four moments of the velocity distribution. At the beginning of the evolution ( $t = 0$ ) the disk has, by construction, the radial dispersion profile given by eq. (12).

Our initial model for the iterative method was a “cold” disk where all particles move on circular orbits (see previous section where we constructed DISK.SVR). We made 100 iterations, each with  $t_i = 20$ . Note that this is twice the number of iterations used for DISK.SVR, because the converge in the case of line-of-sight kinematics is slower. The remaining parameters were taken  $dt = 1/2^4$ ,  $\epsilon = 0.04$  and  $\theta_t = 0.9$ . In order to fix the profile of  $\bar{v}_{\text{los}}(x)$  (for DISK.MVLOS) and the profile of  $\sigma_{\text{los}}(x)$  (for DISK.SVLOS) we used the algorithms described in section 2.3.3. The number of layers in these algorithms was  $n_{\text{div}} = 200$ .

Let us check the equilibrium of the DISK.MVLOS and the DISK.SVLOS disks. In both cases we use the halo and bulge constructed in the previous section, because the mass model is the same. For the self-consistent evolution we used the same parameters as in previous section. The evolution of the disks in these models is illustrated in figures 11 and 12, respectively. These show that the constructed disks are as close to equilibrium as they should.

It is interesting to compare DISK.SVR and the two disks constructed from it by using line-of-sight kinematics. The three radial profiles of  $\sigma_R$  and  $\sigma_{\varphi}$  are visibly different, as can be seen in figure 13. The velocity dispersion in the disk plane is visibly bigger for DISK.MVLOS than for DISK.SVR, especially near the disk periphery. This is also the case for DISK.SVLOS, but to a lesser extent. In general, it is clear that both models DISK.MVLOS and DISK.SVLOS are different from DISK.SVR. This was not expected and must be due to the fact that more than one equilibrium solution exists for the adopted constraints. This must be kept in mind when we apply our method for constructing phase models of real galaxies and we will discuss it more extensively in a forthcoming paper.

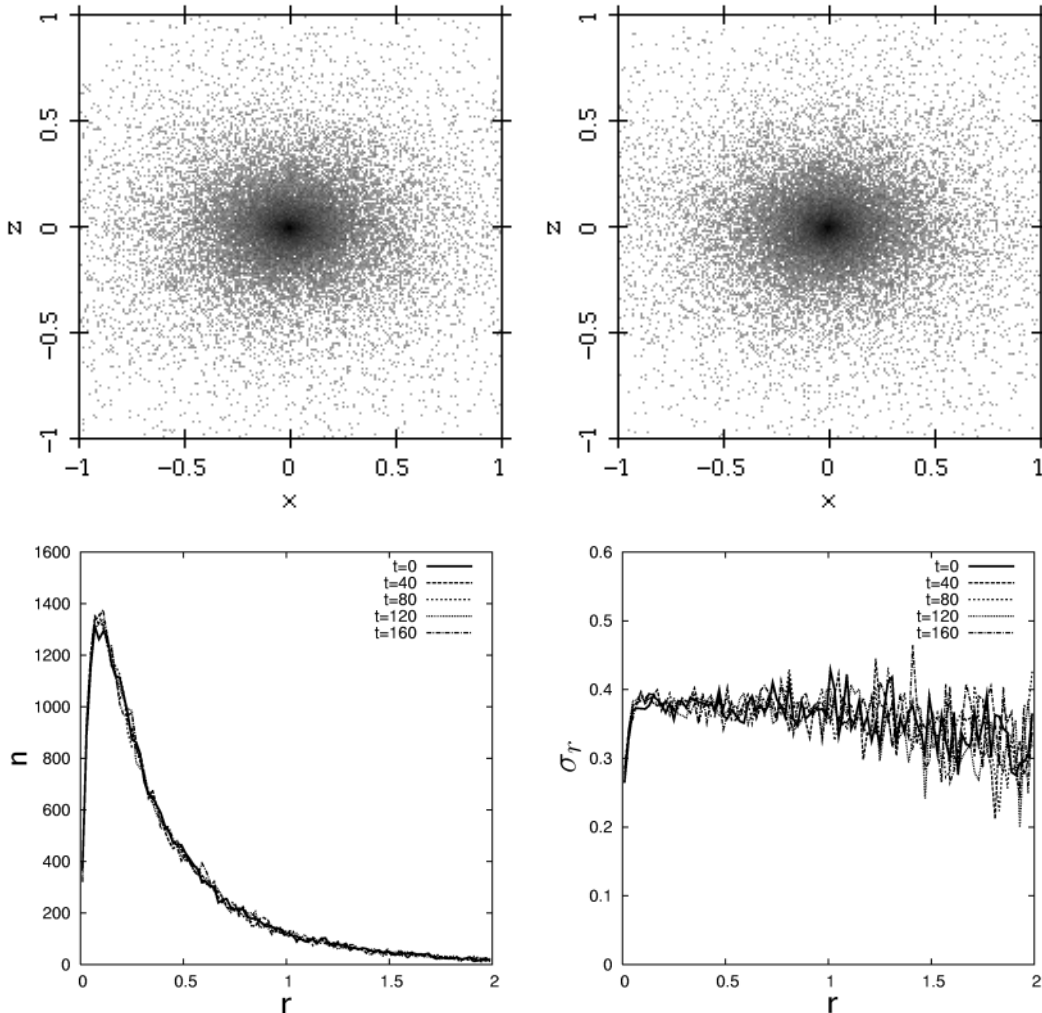


**Figure 7.** Initial evolutionary stages for the bulge of the constructed disk galaxy model. The evolution of the model was calculated with live disk, halo, and bulge (see also fig. 6 and 8). The upper snapshots show the bulge viewed edge-on for two moments of time (0, 160); the grey intensities correspond to the logarithms of particle numbers in the pixels. The bottom panels show the dependence of two parameters of the bulge on the spherical radius  $r$  for various moments of time. Here  $n$  is the number of particles in concentric spherical layers;  $\sigma_r$  is the velocity dispersion in the  $r$  direction (in spherical coordinate system). We demonstrate these parameters in order to show that the model is close to the equilibrium. For astrophysical applications it should be taken into account that the bulge in our model is not spherical.

#### 4 CONCLUSIONS

We presented a new method for constructing equilibrium phase models for stellar systems — the iterative method. The aim of this method is to construct equilibrium  $N$ -body models with given parameters, or constraints. More specifically, these are a given mass distribution and, if desired, given kinematic properties, parameters, or constraints. Our method is straightforward both conceptually and in its implementation. We believe that it is this simplicity that makes this method so powerful. It simply relies on a constrained, or guided evolution. We let the system reach equilibrium via a dynamical evolution in a number of successive steps. In between two such steps we make sure that the parameters are set to their desired value and/or that the constraints are fulfilled. This means that the evolution is guided towards an equilibrium with the desired parameters and/or constraints.

Setting a mass distribution is of course obligatory, but kinematical constraints are not. If we wish to include them, we have the choice of a large number of possibilities, such as setting the radial profile(s) of one, or more moments of the velocity distribution. In this article we described only a few types of kinematic constraints: the profile of radial velocity dispersion, the profile of velocity anisotropy, a condition of velocity isotropy and line-of-sight kinematics. Procedures for further types of kinematic constraints can be easily found following similar techniques. Furthermore, our implementation of the iterative method can be directly applied to systems with arbitrary geometry, i.e. the given mass distribution can be arbitrary and need not have any symmetries. Thus our method can be used in many different applications.

We used our iterative method to construct several models. The first one is a triaxial system. The second one is

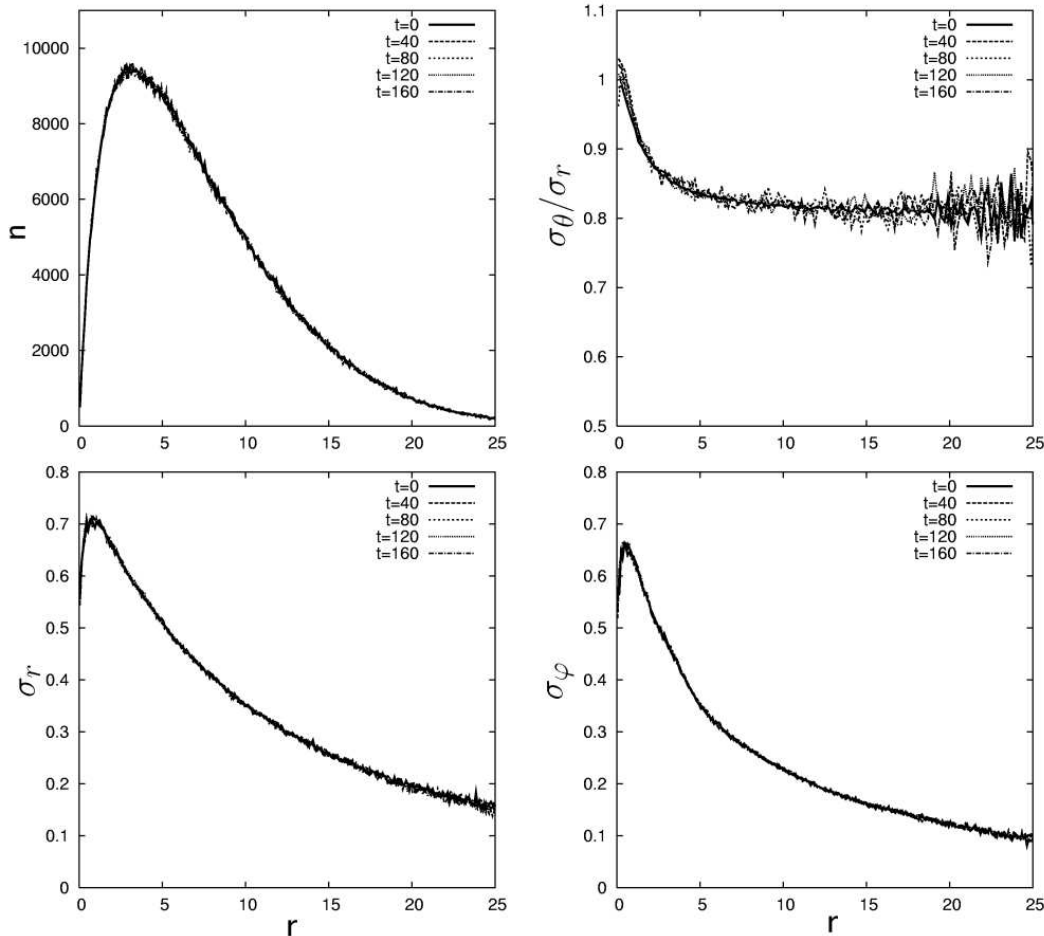


**Figure 8.** Initial evolutionary stages for the halo of the constructed disk galaxy model. The evolution of the model was calculated with live disk, halo, and bulge components (see also fig. 6 and 7). We show the dependence of various halo parameters on the spherical radius  $r$  for various moments of time. Here  $n$  is the number of particles in concentric spherical layers (upper left panel);  $\sigma_\theta/\sigma_r$  is the ratio of velocity dispersion in the  $\theta$  and  $r$  directions (upper right panel);  $\sigma_r$  is velocity dispersion in the radial direction (bottom left panel);  $\sigma_\varphi$  is the velocity dispersion in the  $\varphi$  direction (bottom right panel). At the initial moment of time the halo has the profile of  $\sigma_\theta/\sigma_r$  given by (13).

a multi-component model of a disk galaxy consisting of a stellar disk with a given radial velocity dispersion profile, a non-spherical bulge and a halo with a given anisotropy profile. We also constructed two disk models with given line-of-sight kinematic. Using self-consistent  $N$ -body simulations, we made sure that the models we constructed are indeed very close to equilibrium (see figs. 3, 6, 7, 8, 12 and 11).

The iterative method has a number of further applications. It can of course be used for constructing equilibrium initial conditions for  $N$ -body modelling of stellar systems. For instance, the iterative method allows one to investigate bar formation in galaxies with a halo having different kinematics. Also the iterative method can be applied for constructing phase models of real galaxies. For example, we can model observational data by constructing phase models with given line-of-sight kinematics, as shown in section 3.3. This paves the way for studies of e.g. the distribution of dark matter in ellipticals, or obtaining phase space models of observed disk galaxies. A further interesting application is the

study of the properties of several equilibrium models for a given mass distribution, as for example triaxial systems.

The software necessary for the implementation of this method should be thought of in a very modular way, e.g. with different units for the various kinematical constraints, and is very straightforward to write. Nevertheless, we will make our own software publicly available as soon as this paper is accepted, at the address <http://www.astro.spbu.ru/staff/seger/soft/>. This package will contain also step-by-step examples for constructing models by using the iterative method, including the models described in this article. Our software uses the  $N$ -body code *gyrfalcon* (Dehnen 2000, 2002) and the *NEMO* package (<http://astro.udm.edu/nemo>; Teuben 1995).

## ACKNOWLEDGEMENTS

We thank the referee, J. Dubinski, for helpful comments.

This work was partially supported by grants ANR-06-BLAN-0172 and ANR-XX-BLAN-XXXX, by the Russian

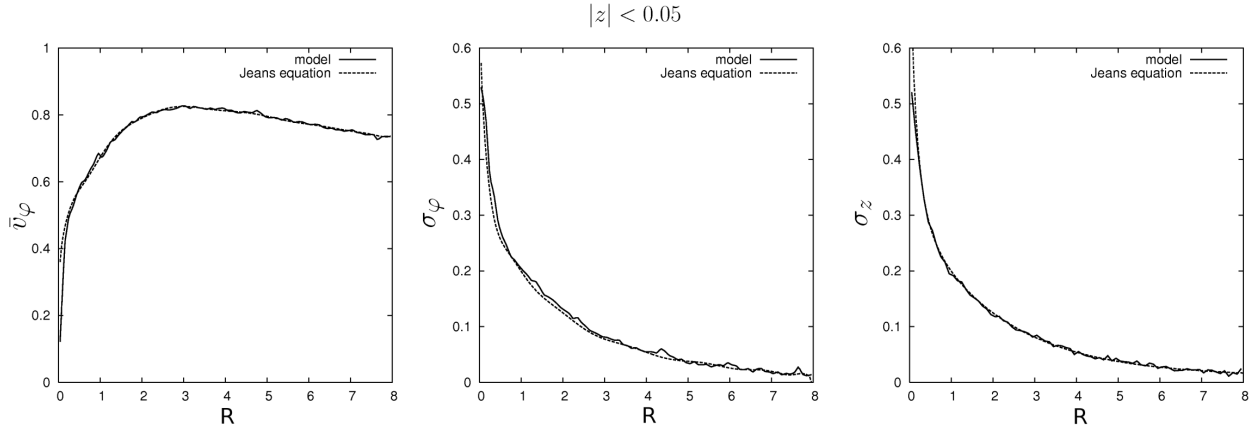


**Figure 9.** Comparison of profiles of the velocity distribution moments calculated from the Jeans equations and from the disk of the constructed disk galaxy model (DISK.SVR). All moments for the disc were calculated inside the region  $|z| < 0.05$ . Left panel: the solid line corresponds to the value  $\bar{v}_\varphi$  for the model, and the dashed line corresponds to the same value calculated from the Jeans equation (the first equation of the system (14)) for  $z = 0$ , and where the values  $\sigma_R$  and  $\sigma_\varphi$  were taken from the model. Middle panel: the solid line corresponds to the value  $\sigma_\varphi$  for the model, and the dashed line corresponds to the same value calculated from the Jeans equation (the second equation of the system (14)), where the values  $\bar{v}_\varphi$  and  $\sigma_R$  were taken from the model. Right panel: the solid line corresponds to the value  $\sigma_z$  for the model, and the dashed line corresponds to the same value calculated from the Jeans equation (the third equation of the system (14)).

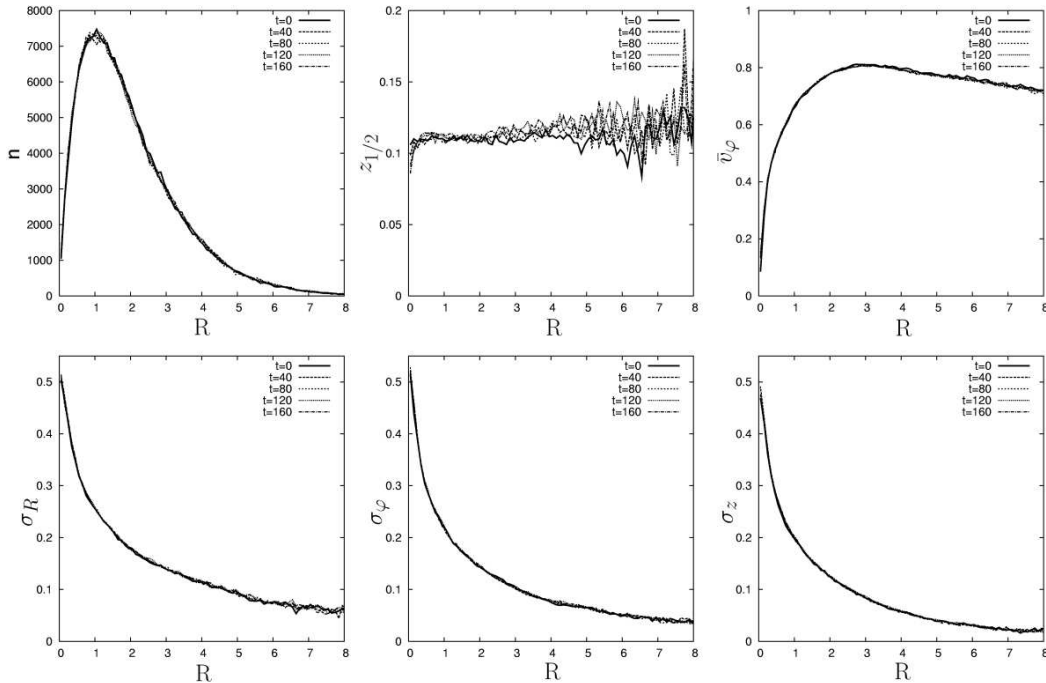


**Figure 11.** Initial evolutionary stages for the model DISK.MVLOS. The evolution of the model was calculated with live disk, halo, and bulge components (we used the halo and bulge constructed in section 3.2). The same values are shown as in middle and bottom panels of Fig. 6.

Foundation for Basic Research (grants 06–02–16459 and 08–02–00361a) and by a grant from the President of the Russian Federation for support of Leading Scientific Schools (grant NSh-8542.2006.02).

## REFERENCES

- Athanassoula E., 2007, *MNRAS*, 377, 1569  
 Athanassoula E., Fady, E., Lambert J. C., Bosma A., 2000, *MNRAS*, 314, 475  
 Athanassoula E., Sellwood J. A., 1986, *MNRAS*, 213, 232  
 Barnes J., 1988, *ApJ*, 331, 699

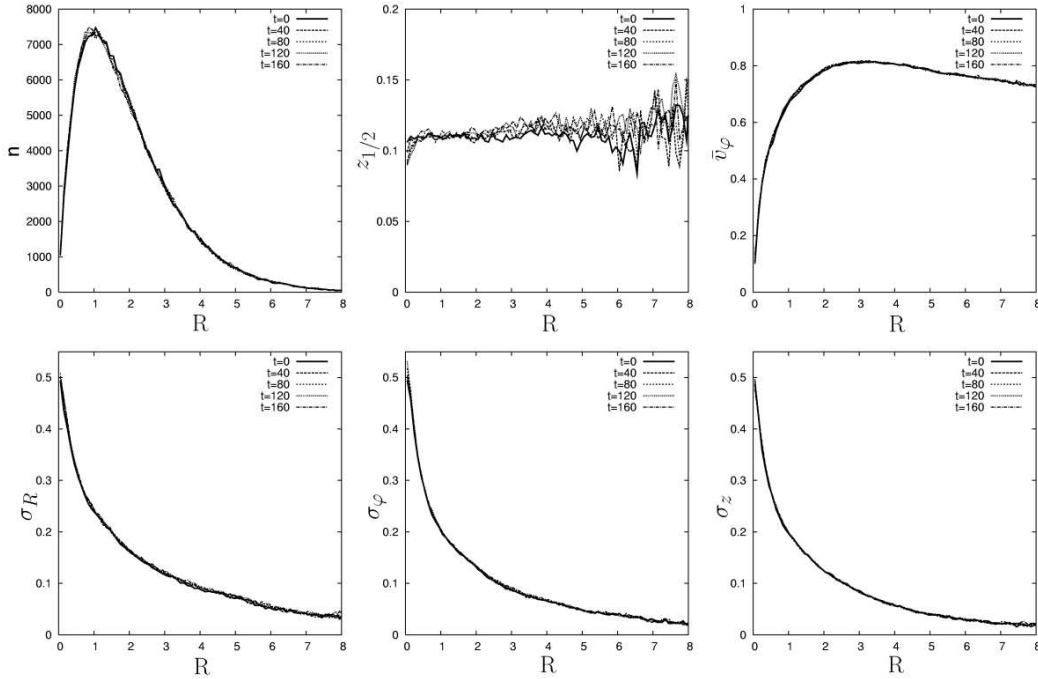


**Figure 12.** Initial evolutionary stages for the model DISK.SVLOS. The evolution of the model was calculated with live disk, halo, and bulge components (we used halo and bulge constructed in section 3.2). The same values are shown as in middle and bottom panels of Fig. 6.

Binney J., Tremaine S., 1987, Galactic Dynamics. Princeton Univ. Press, Princeton  
 de Lorenzi et al., 2008, MNRAS, 385, 1729  
 Dehnen W., 2000, ApJ, 536, 39  
 Dehnen W., 2002, Journal of Computational Physics, 179, 27  
 Häfner R., Evans N. W., Dehnen W., Binney J., 2000, MNRAS, 314, 433  
 Hernquist L., 1990, ApJ, 356, 359  
 Hernquist L., 1993, ApJS, 86, 389  
 Kuijken K., Dubinski J., 1995, MNRAS, 277, 1341  
 McMillan P.J., Dehnen W., 2007, MNRAS, 378, 541  
 Navarro J.F., Frenk C.S., White S.D.M., 1996, ApJ, 462, 563  
 Rodionov S.A., Sotnikova N.Ya., 2005, Astron. Rep., 49, 470  
 Rodionov S.A., Sotnikova N.Ya., 2006, Astron. Rep., 50, 983  
 Rodionov S.A., Orlov V.V., 2008, MNRAS, 385, 200  
 Schwarzschild M., 1979, ApJ, 232, 236  
 Sotnikova N.Ya., Rodionov S.A., 2006, Astron. Lett., 32, 649  
 Sotnikova N.Ya., Rodionov S.A., 2008, Astron. Lett., accepted  
 Teuben P.J., 1995, in “Astronomical Data Analysis Software and Systems IV”, ed. Shaw R. A., Payne H. E., Hayes J. J. E., ASP Conf. Ser. Vol. 77, 398  
 Thomas, J. et al., 2007, MNRAS, 382, 657  
 A. Toomre, 1964, ApJ, 139, 1217  
 van den Bosch R. C. E., van de Ven G., Verolme E. K., Cappellari M., de Zeeuw P. T., 2008, MNRAS, 385, 647  
 van den Bosch R. C. E., de Zeeuw T., Gebhardt K., Noyola

E., van de Ven G., 2006, ApJ, 641, 852  
 Widrow L.M., Dubinski J., 2005, ApJ, 631, 838  
 Zang T. A., 1976, Unpub. PhD thesis, MIT

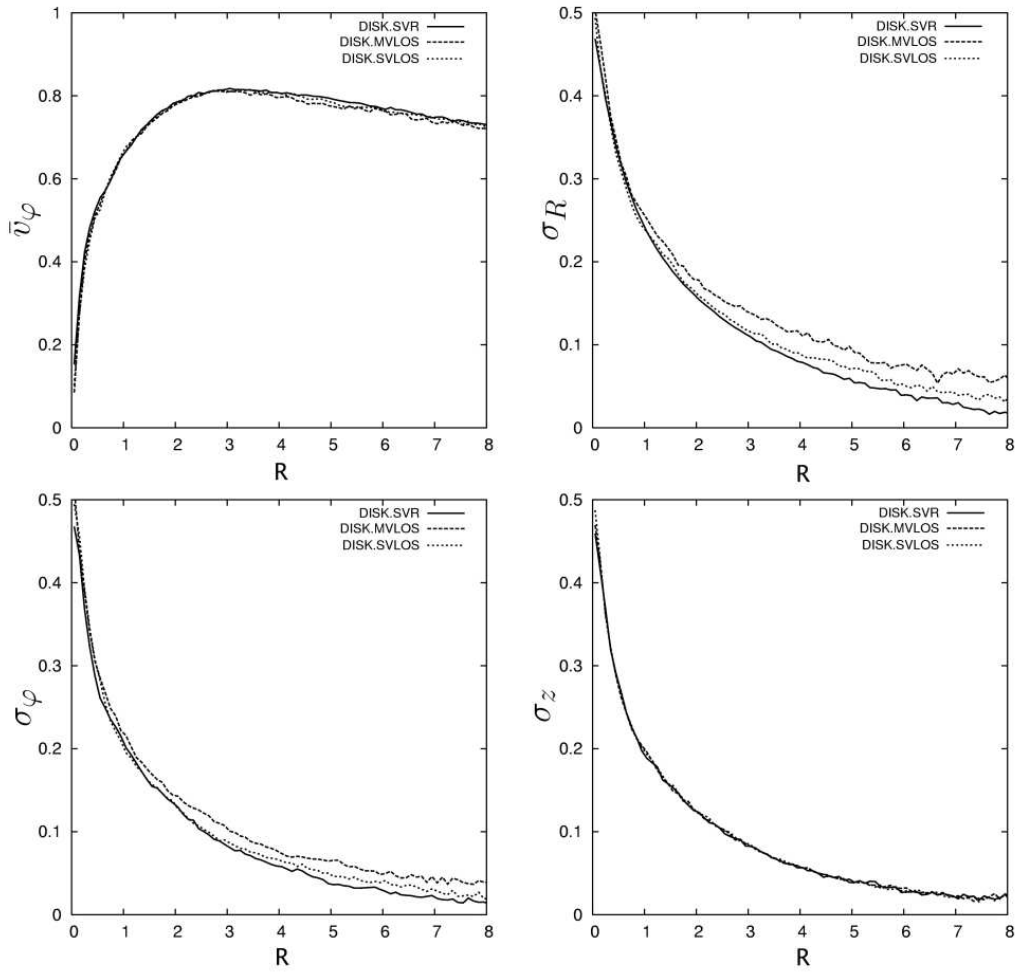


**Figure 13.** The dependence of four moments of the velocity distribution, namely  $\bar{v}_\varphi$ ,  $\sigma_R$ ,  $\sigma_\varphi$  and  $\sigma_z$  as a function of the cylindrical radius  $R$  for DISK.SVR, DISK.MVLOS and DISK.SVLOS.